

# Using Lyman- $\alpha$ to detect galaxies that leak Lyman continuum

Anne Verhamme<sup>1</sup>, Ivana Orlitová<sup>1,2</sup>, Daniel Schaerer<sup>1,3</sup>, Matthew Hayes<sup>4</sup>.

<sup>1</sup> Observatoire de Genève, Université de Genève, 51 Ch. des Maillettes, 1290 Versoix, Switzerland

<sup>2</sup> Astronomical Institute, Academy of Sciences of the Czech Republic, Boční II 1401, 141 00 Prague, Czech Republic

<sup>3</sup> CNRS, IRAP, 14 Avenue E. Belin, 31400 Toulouse, France

<sup>4</sup> Department of Astronomy, Oskar Klein Centre, Stockholm University, AlbaNova University Centre, SE-106 91 Stockholm, Sweden

Received date / Accepted date

## ABSTRACT

**Aims.** We propose to infer the output of the ionising continuum-leaking properties of galaxies based upon their Ly $\alpha$  line profiles.

**Methods.** We carried out Ly $\alpha$  radiation transfer calculations in two models of H II regions. These models are porous to ionising continuum escape: 1) we define Lyman-continuum (LyC) optically thin star clusters, in which massive stars produce enough ionising photons to keep the surrounding interstellar medium transparent to the ionising continuum, in other words, almost totally ionised, and 2) we define riddled ionisation-bounded media that are surrounded by neutral interstellar medium, but have holes, which results in a covering fraction lower than unity.

**Results.** The Ly $\alpha$  spectra that emerge from these configurations have distinctive features: 1) a classical asymmetric redshifted profile in the first case, but with a small shift of the profile maximum compared to the systemic redshift ( $v_{\text{peak}} \leq 150 \text{ km s}^{-1}$ ); 2) a main peak at the systemic redshift in the second case ( $v_{\text{peak}} = 0$ ), with a non-zero Ly $\alpha$  flux bluewards of the systemic redshift as a consequence. If in a galaxy that leaks ionising photons the Ly $\alpha$  component that emerges from the leaking star cluster(s) is assumed to dominate the total Ly $\alpha$  spectrum, the Ly $\alpha$  shape may be used as a pre-selection tool for detecting LyC-leaking galaxies in objects with high spectral resolution Ly $\alpha$  spectra ( $R \geq 4000$ ). Our predictions are corroborated by examination of a sample of ten local starbursts with high-resolution HST/COS Ly $\alpha$  spectra that are known in the literature as LyC leakers or leaking candidates.

**Conclusions.** Observations of Ly $\alpha$  profiles at high resolution are expected to show definite signatures revealing the escape of Lyman-continuum photons from star-forming galaxies.

**Key words.** Radiative transfer – Reionisation – Galaxies: ISM – ISM: structure, kinematics and dynamics

## 1. Introduction

Determining the population of objects that reionised the Universe and maintained the subsequent thermal history of the intergalactic medium (IGM) remains an outstanding and urgent question in observational cosmology. Observations show that some active galactic nuclei were in place almost at the reionisation epoch, but their numbers were grossly insufficient to reproduce the necessary background of Lyman-continuum (LyC;  $< 912\text{\AA}$ ) radiation (e.g. Cowie et al. 2009; Fontanot et al. 2012). This leaves star-forming galaxies to reionise the Universe, and, while they undoubtedly are in place at the relevant epoch, with hints for a steep luminosity function (LF) at the faint end (Alavi et al. 2014), it still appears that the current populations are insufficient to have completed reionisation by  $z \approx 6$  (e.g. Robertson et al. 2013, and references therein).

Moreover, simply knowing that galaxies are in place is not sufficient: they must also emit enough LyC radiation. In the very nearby Universe this is manifestly not the case, where spaceborne UV telescopes such as the HUT (Hopkins Ultraviolet Telescope) and FUSE (Far Ultraviolet Spectroscopic Explorer) have reported a large number of upper limits (e.g. Leitherer et al. 1995; Heckman et al. 2001; Deharveng et al. 2001; Grimes et al. 2009) and only a small number of weak detections with escape fractions of only a few percent (e.g. Leitet et al. 2011, 2013; Borthakur et al. 2014). Despite the much larger samples of galaxies that have been studied in LyC at  $z \sim 1$  with the Galaxy

Evolution Explorer (GALEX) and the Hubble Space Telescope (HST), the situation still does not change much, and still no individual LyC-leaking galaxies are reported (Malkan et al. 2003; Siana et al. 2007; Cowie et al. 2009; Siana et al. 2010).

The beginnings of the necessary evolution seem to set in at higher redshifts of  $z \sim 3$ . LyC emission has been reported in large samples of Lyman break galaxies (LBGs) and Ly $\alpha$ -emitters (LAEs), using both spectroscopic (Steidel et al. 2001; Shapley et al. 2006) techniques and narrowband imaging bluewards of the restframe Lyman limit (Iwata et al. 2009; Nestor et al. 2011, 2013; Mostardi et al. 2013). Curiously, most narrowband images of the emitted LyC show spatial offsets from the non-ionising UV continuum, which may indeed be consistent with models of LyC leakage being facilitated by supernova winds (Clarke & Oey 2002) or unresolved galaxy mergers (Gnedin et al. 2008). Alternatively, the spatial offsets may also be explained by projected galaxies at lower redshift that contaminate the observed LyC (Vanzella et al. 2010, 2012), although simulations performed by Nestor et al. (2013) suggest that this probably does not account for all detections.

Another particularly relevant result from  $z \sim 3$  is that LyC leakage seems to be stronger from LAEs than from LBGs. Theorists have repeatedly shown that LyC leakage generally increases at lower galaxy masses (e.g. Ferrara & Loeb 2013; Yajima et al. 2011; Wise & Cen 2009), which superficially seems to be consistent with the stronger LyC leakage found from  $z \sim 3$  LAEs, which tend to occupy lower mass haloes (Ouchi et al. 2005; Gawiser et al. 2006; Guaita et al. 2011). Because the UV LFs found

Send offprint requests to: anne.verhamme@unige.ch

in the high- $z$  Universe are particularly steep (Alavi et al. 2014; Dressler et al. 2014) and LyC escape fractions increase moving downwards across the galaxy LF, the case may indeed be that faint Ly $\alpha$ -emitting galaxies were the main contributors to reionisation. The evolution of the number of Ly $\alpha$  emitting galaxies among the population of LBGs with a sudden drop at  $z > 6$  (Stark et al. 2010; Ono et al. 2012; Schenker et al. 2014) is usually interpreted as due to an increase of the neutral fraction of the IGM. But if Ly $\alpha$ -emitting galaxies have a non-negligible LyC escape fraction ( $\geq 15\%$ ) at  $z > 6$  and if this increases again towards higher  $z$ , then these galaxies become fainter in Ly $\alpha$  at levels that could (partially) mimic a reionisation signature (Hayes et al. 2011; Dijkstra et al. 2014). This reasoning can be generalised to all nebular lines: along the same idea, Zackrisson et al. (2013) proposed to search for weak nebular lines in the spectra of galaxies of the reionisation epoch as a probe for LyC leakage. In the local Universe, Lee et al. (2009) observed a systematic underestimate of the star formation rate derived from H $\alpha$  luminosity, SFR(H $\alpha$ ), compared to SFR(UV), the star formation rate derived from ultraviolet luminosity, in dwarf galaxies among their sample of nearby galaxies, which can be interpreted as the result of a higher escape of ionising photons in smaller galaxies.

To explain the low success rate of LyC-leaking detections, the commonly invoked explanation is that the galaxies responsible for reionisation are the faintest ones, which are below our current continuum detection threshold (e.g. Ouchi et al. 2008). On the other hand, a huge amount of spectroscopic data are available in Ly $\alpha$ , up to the reionisation redshift (e.g. Shapley et al. 2003; Hu et al. 2010; Stark et al. 2010; Guaita et al. 2010, 2011; Dressler et al. 2011; Bielby et al. 2011; Pentericci et al. 2010, 2011; Kulas et al. 2012; Jiang et al. 2013b,a; Ellis et al. 2013; Schenker et al. 2013). Could we tell from the Ly $\alpha$  line shape if a galaxy is a good candidate for continuum leaking? This is the starting point of our study. Based on Ly $\alpha$  radiation transfer modelling, we first present the theoretically expected Ly $\alpha$  spectral characteristics of continuum-leaking galaxies. We then compare our diagnostics with two other indirect diagnostics of continuum leaking that have been proposed in the literature, which are (a) a low covering fraction of the interstellar absorption lines that are in a low-ionisation state (LIS) (e.g. Heckman et al. 2011; Jones et al. 2013), and (b) a high ratio of [O III] $\lambda$ 5007/[O II] $\lambda$ 3726, 3729 as a proxy for density-bounded H II regions (Nakajima & Ouchi 2014; Jaskot & Oey 2013; Kewley et al. 2013). Finally we compare the different indicators for a sample of low-redshift galaxies.

Our paper is structured as follows. The link between Lyman-continuum leakage and the Ly $\alpha$  line profile is discussed in Sect. 2. In Sect. 3 we compare the different leaking indicators for a sample of low-redshift galaxies. Our main results are discussed in Sect. 4 and are summarised in Sect. 5.

## 2. Link between LyC and Ly $\alpha$

In this section, we describe the possible implications that ionising continuum leakage from a galaxy may have on its Ly $\alpha$  profile, and we discuss the detectability of these spectral features.

### 2.1. Ionising continuum leakage from galaxies

As described in the introduction, galaxies from which ionising photons escape are extremely rare in the local Universe, at least at the observed luminosities. Only three objects are known as

LyC leakers, and their absolute escape fraction<sup>1</sup> is only a few percent (Bergvall et al. 2006; Leitert et al. 2013; Borthakur et al. 2014). The vast majority of known high-redshift galaxies are also opaque to their own ionising radiation, as demonstrated by the success of the well-known Lyman-break selection (as emphasised recently in Cooke et al. 2014). Only a few tens of objects are detected in the LyC (Iwata et al. 2009; Nestor et al. 2011, 2013; Mostardi et al. 2013). A LyC-leaking galaxy has then peculiar rare properties that we describe below.

#### 2.1.1. Two mechanisms of ionising continuum escape

Our framework is the following: we consider that the bulk of ionising photons produced in galaxies arises from young massive stars, and we neglect AGN or external sources (proximate quasar, UV background, etc.). Young star clusters ionise the surrounding ISM, creating H II regions that are usually ionisation bounded, when the size of their birth gas cloud exceeds the Strömgen radius (Strömgen 1939), but that can be density bounded in peculiar cases when their surrounding cloud is not large enough to absorb all the ionising radiation (e.g. Pellegrini et al. 2012). Density-bounded H II regions are leaking LyC photons by definition, with an escape fraction of

$$f_{\text{esc}}(\text{LyC}) = e^{-\tau_{\text{ion}}}, \quad (1)$$

where  $\tau_{\text{ion}} = \sigma(\nu)N_{\text{HI}}$  is the optical depth seen by an ionising photon of frequency  $\nu$ ,  $N_{\text{HI}}$  is the column density of the remaining neutral gas surrounding the star cluster, and

$$\sigma(\nu) = \sigma_{\nu_0}(\nu/\nu_0)^{-3} \quad (2)$$

is the photoionisation cross-section of a hydrogen atom, defined for  $\nu \geq \nu_0$ , where  $\nu_0$  is the ionisation frequency of the hydrogen atom for which the ionisation cross-section is  $\sigma_{\nu_0} = 6.3 \times 10^{-18} \text{ cm}^2$ .

Usually, and for the remainder of this paper,  $f_{\text{esc}}^{\text{LyC}}$  is considered at the Lyman edge, that is, for  $\nu \approx \nu_0$ . This is also the range probed by observations using narrowband (NB) technics at most redshifts.

In addition to the optically thin regime, we consider another scenario for LyC leaking from galaxies (following Zackrisson et al. 2013): the ionising continuum produced by young massive stars in an ionisation-bounded region ( $\tau_{\text{ion}} \gg 1$ ) can escape in some peculiar cases where the covering fraction of the neutral gas surrounding the cluster is not unity. We call this second configuration of LyC escape riddled ionisation-bounded H II regions. The covering fraction, CF, is defined as the fraction of lines of sight that are optically thick to LyC photons. This implies that some lines of sight are transparent to LyC photons and some are not (e.g. Behrens et al. 2014). The escape fraction of the ionising radiation is simply related to the covering fraction of the neutral gas:

$$f_{\text{esc}}(\text{LyC}) = 1 - CF. \quad (3)$$

#### 2.1.2. Link with the Ly $\alpha$ radiation

Ly $\alpha$  radiation is produced by the recombination of hydrogen atoms in these H II regions that surround young star clusters. The quantity of Ly $\alpha$  photons produced in a galaxy is then proportional to the non-escaping fraction of ionising photons (1 -

<sup>1</sup>  $f_{\text{esc}} = f_{\text{esc,rel}} \times 10^{-0.4 \times A_{1500}} = \frac{(f_{1500}/f_{900})_{\text{int}}}{(f_{1500}/f_{900})_{\text{obs}}} \times 10^{-0.4 \times A_{1500}}$ , as defined in Leitert et al. (2013)

$f_{\text{esc}}(\text{LyC})$ ). Almost all LyC leakers that have been reported in the literature have an escape fraction ranging from a few percent – for the few spectroscopically confirmed leakers – to a few tens of percent – from indirect measurement of the covering fraction of low-ionisation state (LIS) absorption lines. They certainly produce copious amounts of Ly $\alpha$  radiation.

A galaxy typically contains several star clusters, which means that a LyC leaker may be a mixture of non-leaking and leaking star clusters, with these two scenarios: either leaking from a LyC optically thin star-forming region, or from an H II region with a low covering fraction. In the following, we first investigate the Ly $\alpha$  spectrum that emerges from LyC optically thin H II regions and the Ly $\alpha$  spectrum that emerges from riddled LyC optically thick regions, both modelled with spherical shells of neutral gas surrounding a Ly $\alpha$  source.

## 2.2. Ly $\alpha$ transfer in a LyC optically thin H II region

We first estimate the optical depth seen by a Ly $\alpha$  photon in a medium that is optically thin for LyC, that is, when  $\tau_{\text{ion}} \lesssim 1$ . The column density of neutral hydrogen along the line of sight is of the order of

$$N_{\text{HI}} = 1/\sigma_{\nu_0} \sim 1.6 \times 10^{17} \text{ cm}^{-2}, \quad (4)$$

corresponding to  $\tau_{\text{ion}} = 1$ . For comparison, the Ly $\alpha$  optical depth at the line centre of such a low column density medium is still

$$\tau_0 = 5.88 \times 10^{-14} (12.85/b) N_{\text{HI}} \sim 10^4 \quad (5)$$

for a Doppler parameter of  $b = 12.85 \text{ km s}^{-1}$ , corresponding to an ISM temperature of  $T = 10^4 \text{ K}$  (e.g. Zheng & Miralda-Escudé 2002).

### 2.2.1. Experimental setup

The formalism developed by Neufeld (1990) is not valid in this peculiar regime where  $\sqrt{\pi}\tau_0 \leq 10^3/a$ , with  $\tau_0$  the Ly $\alpha$  optical depth at the line centre and  $a$  the ratio between the natural to Doppler broadening, as illustrated for example in Fig. 2 of Verhamme et al. (2006). Numerical experiments are necessary to study Ly $\alpha$  radiation transfer in such low optical depth regimes. Assuming that H II regions are cavities of ionised gas that contain young stars and are surrounded by neutral gas, we simulated the Ly $\alpha$  transfer with our Monte Carlo code *McLy $\alpha$*  (Verhamme et al. 2006; Schaerer et al. 2011) through the same geometrical configurations as previously published: spherical shells of homogeneous neutral gas that are characterised by four physical parameters,

- the radial expansion velocity  $v_{\text{exp}}$ ,
- the radial column density  $N_{\text{HI}}$ ,
- the Doppler parameter  $b$ , encoding thermal and turbulent motions, and
- the dust absorption optical depth  $\tau_d$ , linked to the extinction by  $E(B - V) \sim (0.06 \dots 0.11)\tau_d$ .

The lower numerical value corresponds to an attenuation law for starbursts according to Calzetti et al. (2000), the higher value to the Galactic extinction law from Seaton (1979). However, the exact geometry that we consider is not important. We tested that our main results, which we detail below, are not altered by other simple geometries such as a sphere or a slab.

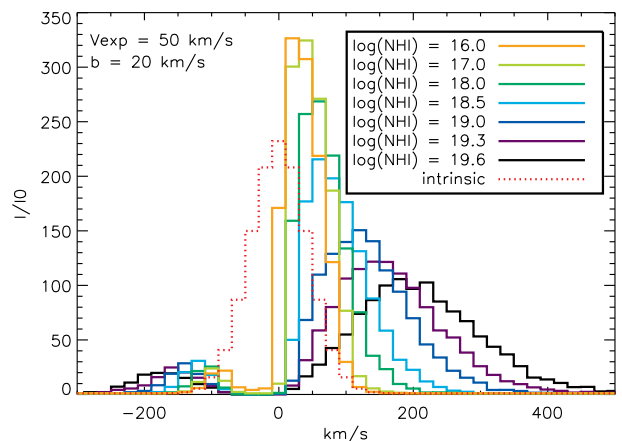


**Fig. 1.** Spectra emerging from starbursts with neutral column densities ranging from the LyC optically thin regime ( $N_{\text{HI}} \leq 10^{17} \text{ cm}^{-2}$ ) to  $N_{\text{HI}} = 10^{19.6} \text{ cm}^{-2}$ , as an illustration of the line broadening with increasing optical depth. The models are dust free, with an expansion velocity  $v_{\text{exp}} = 50 \text{ km s}^{-1}$ , and a Doppler parameter  $b = 20 \text{ km s}^{-1}$ . The intrinsic spectrum is a flat continuum plus a Gaussian emission line of  $FWHM = 100 \text{ km s}^{-1}$  and  $EW = 100 \text{ \AA}$ . These spectra are not convolved to account for a finite instrumental resolution, but they would correspond to extremely high-resolution spectra ( $R \geq 15000$  or  $\Delta\nu \leq 20 \text{ km s}^{-1}$ ). In this plot and in the following theoretical spectra, the notation  $I/I_0$  indicates that the profiles are normalised to the flux level in the continuum,  $I_0$ , which is the mean number of escaping photons per frequency bin over an arbitrary frequency range far from line centre, here  $xr = [-3000 \text{ km s}^{-1}; -2000 \text{ km s}^{-1}]$ .

### 2.2.2. Results: identifiable features in the Ly $\alpha$ spectrum

Ly $\alpha$  radiation transfer in such a low optical depth medium is characterised by extremely narrow line-profiles, as illustrated in Fig. 1, where we compare emerging Ly $\alpha$  spectra from expanding shells of increasing optical depth. The intrinsic spectrum is a Gaussian emission line of  $FWHM = 100 \text{ km s}^{-1}$  and  $EW = 100 \text{ \AA}$ . The shells are homogeneous, isothermal ( $b = 20 \text{ km s}^{-1}$ ), and dust free, and the expansion velocity is  $50 \text{ km s}^{-1}$ . The shift and broadening of the profile is clearly visible when the column density increases. Extremely narrow Ly $\alpha$  profiles ( $FWHM \sim 200 \text{ km s}^{-1}$ ), with a peak shifted by less than  $\sim 150 \text{ km s}^{-1}$  compared to the systemic redshift of an observed galaxy, are therefore good candidates for LyC leaking through the LyC optically thin scenario.

In the left panel of Fig 2, the offset between the profile maximum and the centre of the restframe Ly $\alpha$  line versus the neutral column density for a sample of shell models extracted from the library described in Schaerer et al. (2011), with moderate Doppler parameter ( $10 < b < 40 \text{ km s}^{-1}$ ), and moderate extinction ( $0 < E(B-V) < 0.2$ ), to restrain our study to Ly $\alpha$  profiles in emission. The global trend is a correlation between  $\log(N_{\text{HI}})$  and  $v_{\text{peak}}$ : when the column density of the shells increases, the peak of the profile is increasingly redshifted away from the line centre, except for high values of the expansion velocity ( $v_{\text{exp}} > 300 \text{ km s}^{-1}$ , red dots in the plot). The reason why models with high outflow velocity have a small shift of the Ly $\alpha$  peak is that a Ly $\alpha$  photon arriving at the fast moving shell will be seen out of resonance, and its probability to cross the shell without interaction is high. For high enough velocities, the intrinsic, unaltered Ly $\alpha$  spectrum would be recovered by the observer.

Figure 2 clearly shows that models with  $N_{\text{HI}} < 10^{18} \text{ cm}^{-2}$  are characterised by  $v_{\text{peak}} < 150 \text{ km s}^{-1}$ . However, it also shows that

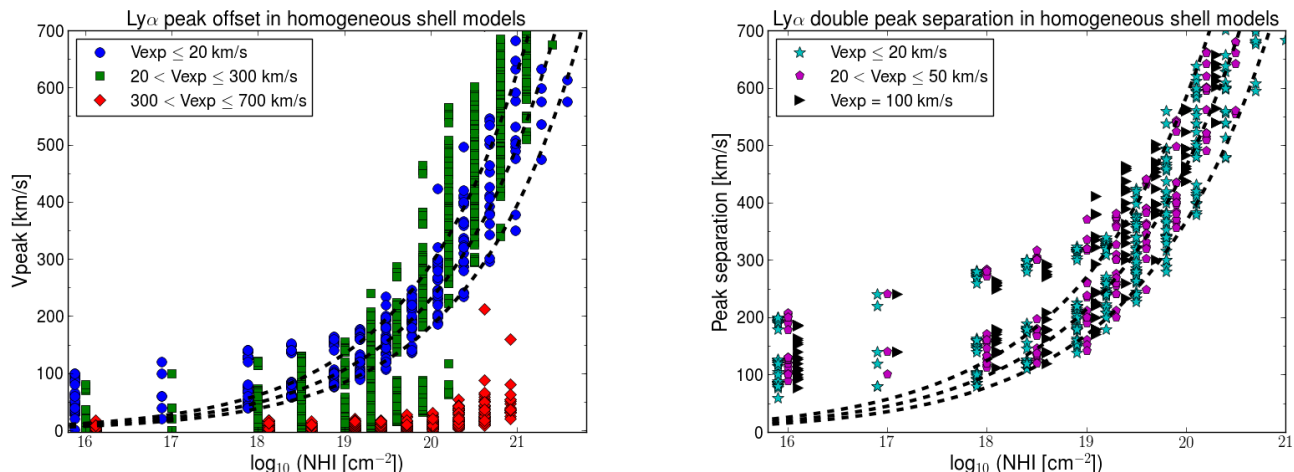


**Fig. 2.** Correlation between the Ly $\alpha$  peak positions and the neutral gas column density as measured in the grid of McLya radiation transfer models in spherical homogeneous shells (Verhamme et al. 2006; Schaerer et al. 2011). **Left:** Ly $\alpha$  peak offset  $v_{\text{peak}}$ . We colour-code three ranges of the outflow velocity: static models in blue, moderate outflow velocity models in green, high-velocity wind models in red. **Right:** Separation  $S_{\text{peak}}$  of peaks in the double-peak Ly $\alpha$  profiles, i.e. those resulting from Ly $\alpha$  radiative transfer in low-velocity outflows (the profiles become single-peaked for velocities higher than 100 km s<sup>-1</sup>). The black curves in both panels depict the analytically derived Ly $\alpha$  peak positions for radiative transfer in a static uniform sphere (Dijkstra et al. 2006). From top to bottom, they correspond to  $b = 40$  km s<sup>-1</sup>,  $b = 20$  km s<sup>-1</sup> and  $b = 10$  km s<sup>-1</sup>. Some discrepancy between the analytical estimate of  $V_{\text{peak}}$  and the numerical experiment is expected at the low N<sub>HI</sub> end, since the analytical solution is only valid in an optically thick regime (see for example Fig.2 in Verhamme et al. 2006). We checked that these results are independent of instrumental resolution.

the low  $v_{\text{peak}}$  is not a sufficient condition for identifying a LyC leaker, because other effects (high outflow velocities) may cause low  $v_{\text{peak}}$ , too. Nevertheless, Ly $\alpha$  spectra are very useful for *excluding* LyC leakage: a large peak offset,  $v_{\text{peak}} > 150$  km s<sup>-1</sup>, indicates that H<sub>I</sub> column densities are too high to allow LyC escape. In contrast, Ly $\alpha$  spectra with a low  $v_{\text{peak}}$  identify candidates for LyC leakage in optically thin ISM, which need to be confirmed by independent indicators or by direct LyC observation. An estimate of outflow velocities from the blueshift of metallic low-ionisation state (LIS) absorption lines should also be able to distinguish between objects with low  $v_{\text{peak}}$  due to high  $v_{\text{exp}}$ , and objects with a low  $v_{\text{peak}}$  due to a low column density. We verified that the location of  $v_{\text{peak}}$  is not very sensitive to the spectral resolution (see the left panel of Fig. 3). The width of the Ly $\alpha$  peaks would be yet another characteristic that is dependent on the H<sub>I</sub> column density. However, the line width is also affected by spectral resolution, and therefore we provide no selection criteria for this parameter.

The  $v_{\text{peak}}$  reliability critically depends on the redshift precision. We therefore propose a complementary criterion, independent of redshift: in double-peaked Ly $\alpha$  profiles, a small peak separation ( $S_{\text{peak}} < 300$  km s<sup>-1</sup>) is a good tentative indication of transfer in a medium with a low column density, as illustrated in the right panel of Fig. 2. Similar to the  $v_{\text{peak}}$  prediction,  $S_{\text{peak}}$  increases with  $N_{\text{HI}}$ , and a peak separation  $> 300$  km s<sup>-1</sup> rules out a low optical depth of the ionising radiation. However,  $S_{\text{peak}} < 300$  can exist for  $N_{\text{HI}}$  as high as  $10^{20}$  cm<sup>-2</sup>. A small peak separation is a good indication of a low column density, but not a definitive probe of LyC leaking. Although the method is simple, it holds only for double-peaked spectra, which appear in static to slowly expanding media:  $v_{\text{exp}} \leq 100$  km s<sup>-1</sup> from our library. Synthetic spectra with higher  $v_{\text{exp}}$  have a weak blue peak, which diminishes as  $v_{\text{exp}}$  increases (see the right panel in Fig 3).

We identify a potential difficulty when using this prediction on observed spectra with unknown redshift: the peaks are supposed to be at each side of the line centre, which is not always the case according to the sample of Kulas et al. (2012). Furthermore, some observed spectra have complex substructures (bumps or multiple peaks, see Sect. 3), and the main peak location may be difficult to determine.

### 2.2.3. Discussion

High spectral resolution is needed to recover extremely narrow profiles. The actual canonical good spectral resolution at high redshift is typically  $R \sim 3000$  on VLT-FORS or the Mitchell spectrograph (Chonis et al. 2013; Tapken et al. 2007), or even  $R \sim 5000$  with Xshooter on lensed targets (Christensen et al. 2012b,a; Noterdaeme et al. 2012). In the left panel of Fig. 3, we illustrate the broadening of a theoretical Ly $\alpha$  profile that is due to instrumental resolution. The orange sharp profile is the theoretical one, unconvolved, labelled  $R > 15000$  since the binning corresponds to  $\Delta v \leq 20$  km s<sup>-1</sup>. The green curve has been convolved with a Gaussian of  $FWHM = 75$  km s<sup>-1</sup> corresponding to an observation of the orange profile with a spectral resolution of  $R = 4000$ . The peaks are slightly broader, but the shape of the profile is relatively well conserved. The blue profile corresponds to  $R = 2000$ . The two peaks are still identifiable, but much broader; the central absorption disappears, the whole profile is detected in emission. The black curve corresponds to  $R = 1000$ . The peaks are not identifiable anymore, and the spectrum presents a blue bump, or is elongated towards the blue. When the spectral resolution decreases, the location of the main peak of the profile,  $v_{\text{peak}}$ , is rather well conserved. It slightly shifts towards lower values.  $v_{\text{peak}}$  is much less sensitive to the spectral resolution than the peak width or the overall spectral shape.

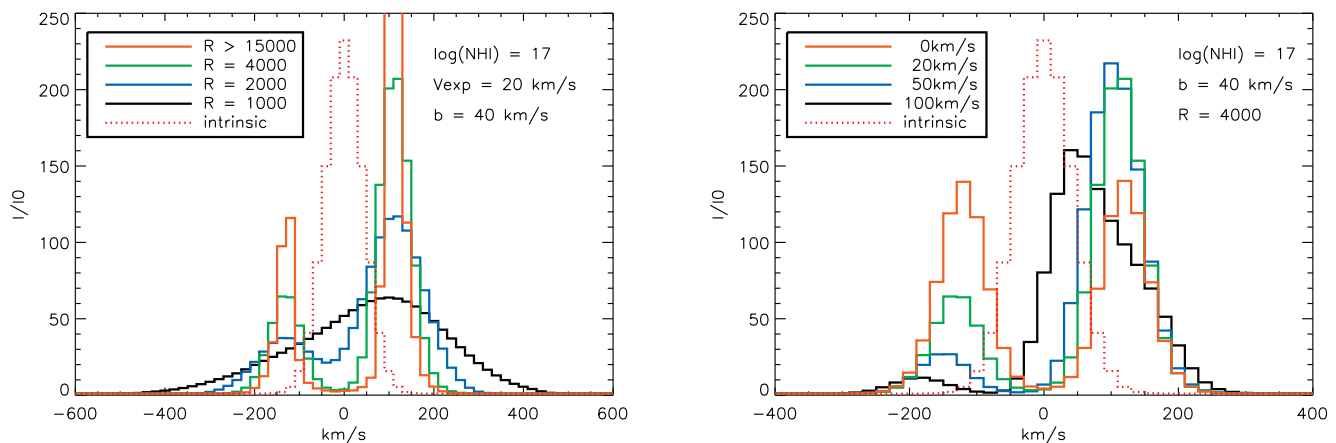


**Fig. 3.** Influence of the spectral resolution (left) and the outflow velocity (right) on the shape of emerging spectra from density-bounded starbursts with low neutral column densities ( $N_{\text{HI}} \leq 10^{17} \text{cm}^{-2}$ ). An observational signature of density-bounded ISM is a small shift of the profile maximum,  $v_{\text{peak}}$ , independent of the expansion velocity  $v_{\text{exp}}$ .

By comparing dust-free and dusty models of density-bounded ISMs, we checked that dust only has a weak effect on the Ly $\alpha$  profiles: the static case is only affected by a global flux reduction, but the double-peaked shape is conserved. When the medium is non-static, the effective Ly $\alpha$  optical depth decreases strongly and the transfer becomes almost insensitive to the dust content. The location of  $v_{\text{peak}}$  does not depend on  $\tau_d$ .

Neutral column densities as low as  $10^{17} \text{cm}^{-2}$  are certainly unusual for the intervening interstellar medium of galaxies. Peculiar lines of sight, aligned by chance with an outflow axis, or peculiar objects, with extremely high ionisation parameters (e.g. blue compact galaxies, green peas, extremely strong emission line galaxies; Cardamone et al. 2009; Izotov et al. 2011; Jaskot & Oey 2013), may present these characteristics, however. Observationally, this high-ionisation parameter can be estimated by measuring the [O III]/[O II] ratio (Nakajima & Ouchi 2014; Jaskot & Oey 2014). A high value of [O III]/[O II] ( $> 10$ ) can result from several factors (Kewley et al. 2013; Stasinska et al. 2015): 1) density-bounded H II regions with reduced outermost [O II] regions; 2) a high-ionisation parameter (the high-ionising flux enhances [O III] relative to [O II]); and 3) a low metallicity. In cases of Ly $\alpha$  transfer through density-bounded regions, we expect both  $v_{\text{peak}} \leq 150 \text{ km s}^{-1}$  and a high [O III]/[O II] ratio.

Another observational piece of evidence for a low column density would be to consider the metallic low-ionisation state absorption lines (e.g. Heckman et al. 2011; Jones et al. 2013). Saturated lines imply a high covering fraction of neutral gas along the line of sight. In contrast, weak or undetected LIS absorption lines may be a good indication for a low column density (Erb et al. 2010; Jaskot & Oey 2014). However, this indicator is very sensitive to spectral resolution as well as metallicity.

### 2.3. Ly $\alpha$ transfer in a riddled ISM

Another scenario to allow Lyman-continuum radiation to escape the ISM of a normal galaxy ( $N_{\text{HI}} \gg 10^{17} \text{cm}^{-2}$ ) would be a partial coverage of star-forming regions with neutral gas. This would also have consequences on the emerging Ly $\alpha$  profiles.

#### 2.3.1. Experimental setup

Detailed studies of Ly $\alpha$  radiation transfer in clumpy media have recently been conducted (Dijkstra & Kramer 2012; Laursen et al. 2013; Duval et al. 2014; Gronke & Dijkstra 2014). They focused on regimes in which the resonant Ly $\alpha$  radiation will escape better than the stellar UV continuum, which suffers from extinction. The main result from these studies is that Ly $\alpha$  can escape from extremely optically thick and dusty media in very particular cases: a rather static ISM, with two phases strongly contrasted in density, and a very high covering fraction of the dense clumps. These studies can be seen as numerical validations of the predictions from Neufeld (1991).

We here consider the same kind of two-phase media, static or not, but with a different focus: we search for Lyman-continuum-leaking regimes, or in other words, for clumpy media with a non-unity covering fraction of the neutral gas ( $CF \leq 98\%$ ), and we observe them along LyC-transparent lines of sight. We here adopted the clumpy medium and spherical geometry described in Duval et al. (2014): the shells were built on a  $128^3$  Cartesian grid, with a minimum (maximum) radius of  $R_{\text{min}} = 49$  ( $R_{\text{max}} = 64$ ), and a filling factor  $FF = 0.23$ , set to best fit the observed mass spectrum of the ISM clumps (Witt & Gordon 2000). For simplicity, we considered here that the density of the interclump medium is zero (“high contrast regime” in Duval et al. 2014), to allow for LyC escape through transparent lines of sight even if in principle the interclump medium could have a residual neutral column density  $N_{\text{HI}} \leq 10^{17} \text{cm}^{-2}$ . These clumpy models are illustrated in Figs. 1 and 2 of Duval et al. (2014). As an example, the mean number of clumps along a sight line is  $\sim 4$  in a medium with  $CF = 0.90$ .

#### 2.3.2. Results: identifiable features in the Ly $\alpha$ spectrum

In clumpy geometries, the spherical symmetry is broken: all lines of sight are not equivalent in terms of LyC escape. Peculiar lines of sight, where the source is aligned with a hole, will emit ionising flux, whereas other directions, where the source is obscured, will not emit any ionising photon. This study focuses on the link between Ly $\alpha$  and LyC escape. In the following, we then con-

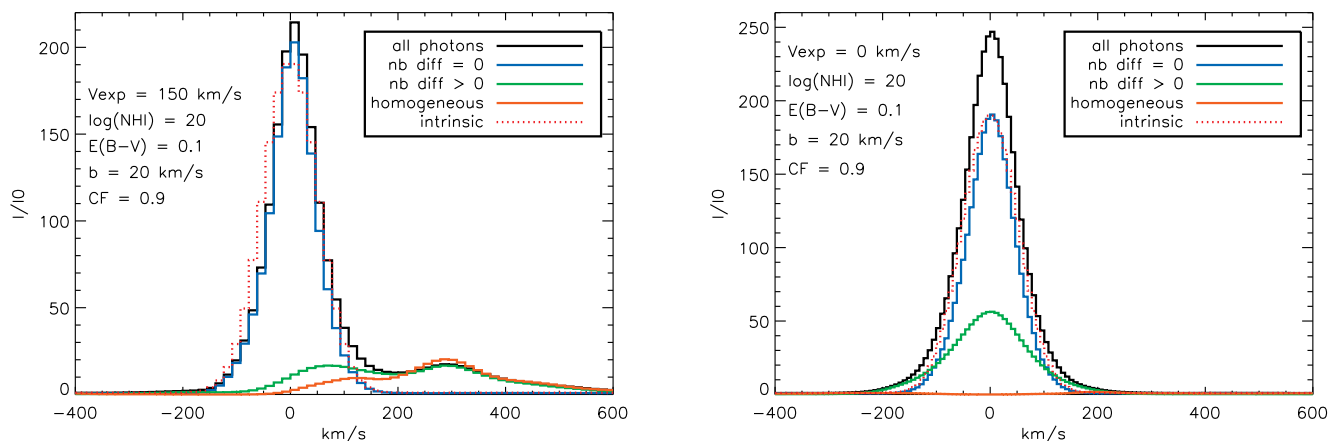


**Fig. 4.** Ly $\alpha$  spectra emerging from clumpy spherical shells with non-unity coverage. **Left:** Expanding shell with fiducial values of the parameters ( $v_{\text{exp}} = 150 \text{ km s}^{-1}$ ,  $\log(N_{\text{HI}}) = 20$ ,  $b = 20 \text{ km s}^{-1}$ ,  $E(B - V) = 0.1$ ). **Right:** Static shell with exactly the same values of the parameters, except the velocity field, which is set to zero. In both cases, the intrinsic spectrum is a continuum plus a Gaussian emission line of  $FWHM = 100 \text{ km s}^{-1}$  and  $EW = 100 \text{ \AA}$  (red dotted line). The black lines shows the global emerging spectra, spatially integrated over the whole shell. The blue and green lines are a decomposition of the black curves in photons that escaped without scattering ( $nb_{\text{diff}} = 0$ , blue) and photons that interacted before escape ( $nb_{\text{diff}} > 0$ , green). This second packet of photons is compared to the result of Ly $\alpha$  radiation transfer in a homogeneous shell (orange curve). These spectra are convolved with a Gaussian to mimic an instrumental resolution of  $R = 4000$ . The main features in the Ly $\alpha$  spectra that emerge from transparent lines of sight in riddled ionisation-bounded H II regions are  $v_{\text{peak}} = 0$  and, as a consequence, a non-zero flux bluewards of the systemic redshift.

sider only Ly $\alpha$  spectra that emerge from LyC transparent lines of sight, that is, with a hole in front of the source.

In Fig. 4, we present the Ly $\alpha$  spectra emerging from clumpy spherical shells with a spatial covering fraction, CF, below unity, observed along a transparent line of sight along which ionising photons can escape. The spectra correspond to high-resolution spectra ( $R=4000$ ). The intrinsic spectrum is a continuum plus a Gaussian emission line of  $FWHM = 100 \text{ km s}^{-1}$  and  $EW = 100 \text{ \AA}$ . In the left panel we show the emerging profile from a clumpy shell with the following fiducial values for the four physical parameters:  $v_{\text{exp}} = 150 \text{ km s}^{-1}$ ,  $\log(N_{\text{HI}}) = 20$ ,  $b = 20 \text{ km s}^{-1}$ , and  $E(B - V) = 0.1$ . These values correspond to the most common best-fit values in our studies fitting observed spectra with our library of homogeneous shells (Verhamme et al. 2008; Dessauges-Zavadsky et al. 2010; Lidman et al. 2012, Orlitová et al. in prep; Hashimoto et al. in prep). We chose  $CF=0.9$  as a fiducial value for the covering factor because it translates into an escape fraction of the ionising continuum of 10%, which corresponds to a high value among the few measurements of LyC escape from galaxies. In the right panel we show Ly $\alpha$  spectra that emerge from a static shell with the same fiducial values except for the expansion velocity, which is set to zero, as well as the profile from a homogeneous shell (orange curve).

As is clear from Fig. 4, the Ly $\alpha$  profiles from transparent sight-lines in a clumpy, spherical shell with a spatial coverage below unity show most of the flux emerging at the line centre (black curve). Behrens et al. (2014) also found the same result: their spectra escaping along lines of sight with holes look very similar to ours, with a very prominent, centred emission (e.g. their Fig. 7). We divided the emerging spectrum from a clumpy medium into two components: 1) the spectrum of photons that did not undergo any scattering before escape ( $nb_{\text{diff}} = 0$ , blue curve), which is identical to the intrinsic spectrum (red dotted line), independently of the geometry or the velocity of the scattering medium, 2) a second component, made of all photons that scattered before escape ( $nb_{\text{diff}} > 0$ , green curve), which will then depend on the geometry and velocity of the scattering medium.

However, this component has a different shape than the spectrum emerging from a shell with the same fiducial values of the parameter, but homogeneous (orange curve). Especially in the static case, the spectrum that emerges from a homogeneous shell shows a broad absorption Voigt profile plus some residual double-peaked emission (orange curve, although the scale is adjusted to see the strong emission peak in other curves, and the absorption feature is barely visible), whereas the spectrum that emerges from the clumpy shell after scattering shows a symmetrical and centred emission line (green curve). We interpret this difference between the green and orange curves seen in both experiments, but enhanced in the static case, as due to Ly $\alpha$  radiation transfer effects: in a medium with holes, resonant photons can bounce on the clumps and find the holes to escape, whereas in the homogeneous medium, they strongly diffuse and increase their chance of being absorbed by dust. Note that the spectrum that emerges along a line of sight without a hole in front of the source will look like the green curve, meaning that it will be only composed of photons having scattered through this clumpy medium.

As a consequence of adding this diffuse component (green curve) to the intrinsic profile, the equivalent width of the spectrum emerging along a LyC transparent line of sight is then always higher than the intrinsic Ly $\alpha$  equivalent width. We therefore predict that Ly $\alpha$  spectra with a peak at the systemic redshift and, as a consequence, a strong Ly $\alpha$  emission and also a non-zero flux bluewards of the Ly $\alpha$  line centre, are good candidates for LyC-leaking objects that leak as a result of a porous ISM. Obviously, partial coverage of neutral gas along the line of sight can also be detected by measuring low-ionisation state (LIS) metal absorption lines (e.g. Jones et al. 2013).

In Fig. 5, we present the effect of spectral resolution on the two diagnostics that we propose (peak at  $v = 0 \text{ km s}^{-1}$  and non-zero flux bluewards of Ly $\alpha$ ) to identify LyC leakers. Although a degradation of the spectral resolution leads to an overestimate of the true emerging flux bluewards of Ly $\alpha$  and  $v_{\text{peak}}$  slightly shifts towards the red, the profiles peak at or close to  $v = 0$  and show

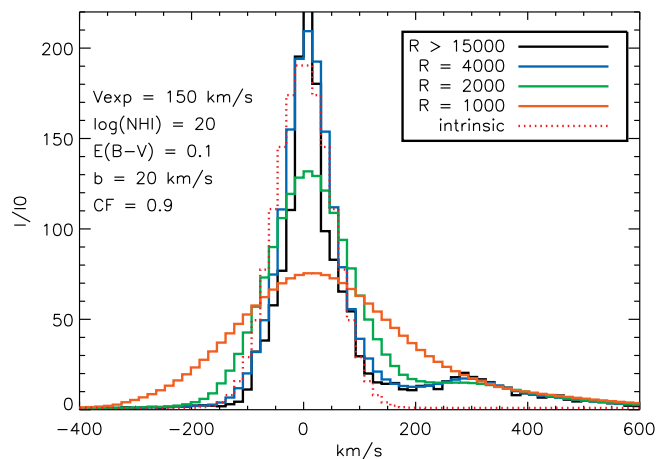


**Fig. 5.** Effects of spectral resolution on the Ly $\alpha$  spectra that emerges from a clumpy shell with fiducial values for the four physical parameters, and a covering fraction of 90%.

a non-zero flux bluewards of  $v = 0$ , quite independently of  $v_{\text{exp}}$ . Hence, our diagnostics for a clumpy Lyman-continuum-leaking ISM are largely independent of the outflow velocity and can be detected with present spectroscopic observations as long as the covering fraction is below unity.

## 2.4. Summary of the link between Ly $\alpha$ and LyC

### 2.4.1. Ly $\alpha$ spectral diagnostic for LyC leakage

We have discussed two cases of LyC leakage: from H II regions with low column densities of neutral gas, and from H II regions with partial coverage of neutral gas. For the first scenario of LyC leakage from density-bounded H II regions, we proposed that observed Ly $\alpha$  spectra with a typical asymmetric redshifted profile are good LyC leaking candidates if the peak of the profile,  $v_{\text{peak}}$ , is within  $150 \text{ km s}^{-1}$  of the systemic redshift. We have shown that this diagnostic is not very sensitive to the spectral resolution. When there is a blue peak in the profile, a peak separation smaller than  $\sim 300(2 \times 150) \text{ km s}^{-1}$  may also be a good indicator for Ly $\alpha$  transfer in media with a low column density ( $\log(N_{\text{HI}}) \leq 18$ ).

For the second scenario of LyC leakage, we claimed that Ly $\alpha$  spectra with a main peak at the systemic redshift of the object, and non-zero flux bluewards of the line centre, are good candidates for continuum leaking. Despite the differences in the geometries studied for instance in Behrens et al. (2014) and here, that is, anisotropic vs. isotropic distributions of gas with a non-unity covering fraction, we reached the same conclusion: lines of sight containing holes lead to Ly $\alpha$  profiles with a prominent peak at the line centre.

### 2.4.2. Limitations of the method

Not all LyC leakers are expected to show this type of Ly $\alpha$  spectra. In particular, the very efficient leakers, with a high escape fraction ( $f_{\text{esc}}(\text{LyC}) \geq 80\%$ ), may have a low Ly $\alpha$  EW, or even no Ly $\alpha$  emission at all when  $f_{\text{esc}} = 1$  (see Fig. 13 in Nakajima & Ouchi 2014), but they may be rare (Vanzella et al. 2010). If most LyC leakers have a moderate  $f_{\text{esc}}(\text{LyC}) \sim 10\%$ , we then predict that their Ly $\alpha$  spectra will be peculiar, as described above.

We did not take into account the effect of IGM attenuation in our modelling. The neutral fraction of the intergalactic medium increases with redshift. The remaining neutral gas in the circumgalactic/intergalactic medium around a galaxy will scatter the light bluewards of Ly $\alpha$  out of the line of sight. The IGM transmission has been predicted to reach a minimum near line-centre (Laursen et al. 2011), which may alter the line shape by artificially redshifting the peak. This effect may complicate the usage of this method at high redshift. However, if they are detected, high-redshift Ly $\alpha$  spectra with small  $v_{\text{peak}}$  will be the best candidates for continuum leaking.

Other configurations or physical processes, such as clumpy geometries with CF=1 in the peculiar Neufeld scenario, high outflow velocities, fluorescence, or gravitational cooling could lead to the same Ly $\alpha$  profiles without leaking. Laursen et al. (2013) and Duval et al. (2014) discussed in detail the conditions of appearance of an enhancement of Ly $\alpha$  escape compared to the UV (non-ionising) continuum. They argued that the peculiar conditions for boosting Ly $\alpha$  compared to continuum appear improbable in the interstellar medium of galaxies. However, the resulting Ly $\alpha$  profile shown in Fig. 17 in Duval et al. (2014) is a narrow line, perfectly symmetric and centred on  $v = 0$ , similar to our prediction of LyC leaking through the second scenario. But in this case, only Ly $\alpha$  can escape, not LyC, since the covering fraction is unity. A way to distinguish between our scenario of LyC leakage and the unlikely Neufeld scenario would be to consider the LIS absorption lines, which should be saturated, and not blueshifted but centred on the systemic redshift, tracing a static medium with CF=1.

If the expansion velocity of the neutral gas around a starburst reaches high values ( $v_{\text{exp}} > 300 \text{ km s}^{-1}$ , as observed in Bradshaw et al. 2013; Karman et al. 2014), Ly $\alpha$  photons may escape through the neutral shell without scattering, and the main peak of the Ly $\alpha$  profile may be located at or close to the systemic redshift (red points in Fig. 2), but no ionising photons will be able to escape. The precise  $v_{\text{exp}}$  beyond which the shell becomes transparent ( $\tau_0 \sim 1$ ) can be expressed as a function of  $N_{\text{HI}}$ :

$$v_{\text{exp}} = \sqrt{\frac{4.7 \times 10^{-17} N_{\text{HI}}}{\pi}} T_4^{-1/2} b. \quad (6)$$

This equation is valid when  $v_{\text{exp}}/b = x_c > 3$ , and the Hjerting function can be approximated by  $H(x, a) \sim \frac{a}{\sqrt{\pi} x^2}$ . An estimation of this outflow velocity from the blueshift of LIS absorption lines should allow distinguishing between high-velocity or low column density cases.

Cantalupo et al. (2005) and Kollmeier et al. (2010) predicted the Ly $\alpha$  spectra and luminosities emitted by a cloud of neutral gas, enlightened by a close-by quasar, or embedded in the cosmological UV background. The external layers of the gas are ionised by the external source, recombine, and emit Ly $\alpha$ . This process is called Ly $\alpha$  fluorescence. Cantalupo et al. (2012) showed convincing detections of LAEs that are powered by fluorescence. Some of the Ly $\alpha$  spectra observed by Trainor & Steidel (2013) from objects illuminated by a strong quasar show a narrow Ly $\alpha$  profile with a blue bump and a small separation between the peaks (Trainor, private communication). Indeed, in case of fluorescence, the external layer of a cloud of neutral gas is ionised. The optical thickness of this layer will be  $\sim 1$  for ionising radiation, corresponding to a neutral column density of  $N_{\text{HI}} \sim 10^{17} \text{ cm}^{-2}$ . The Ly $\alpha$  photons created by recombination inside this layer will then diffuse in such an optically thin medium and should resemble the spectra described above in our first scenario of LyC leakage. In cases of fluorescence, the exter-

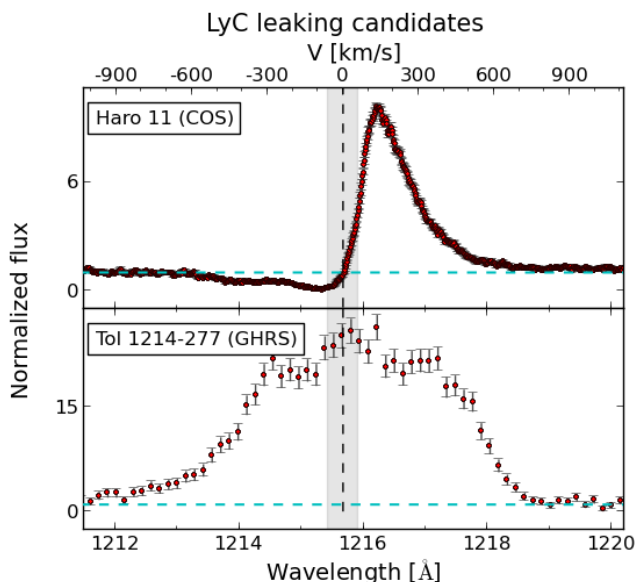


**Fig. 6.** Observed Ly $\alpha$  spectra of LyC leakers from our Ly $\alpha$  criteria. **Top:** HST/COS Ly $\alpha$  profile of the known LyC leaking galaxy Haro 11 Bergvall et al. (2006), with a narrow P Cygni profile with  $v_{\text{peak}} \leq 150 \text{ km s}^{-1}$ , typical of Ly $\alpha$  transfer through low optical depth medium. **Bottom:** GHRs Ly $\alpha$  spectrum of a low-metallicity blue compact dwarf galaxy Tol 1214–277, highly suggestive of Lyman-continuum leakage from a riddled ISM (Sect. 2.3). The systemic redshifts and their errors (grey shaded area in each plot) were adopted from the 6dF survey for Haro 11 and from Pustilnik & Martin (2007) for Tol 1214–277. The blue horizontal line denotes the continuum level.

nal source of ionisation is hopefully either known or bright and hence easily identifiable.

In addition to Ly $\alpha$  emission from gas recombination around starbursts, the other Ly $\alpha$  production channel is via collisional excitation of gas falling onto a halo and converting its gravitational energy to heat through collisions. Ly $\alpha$  emission is the main process for this almost pristine gas to cool. However, the Ly $\alpha$  spectra observed from Ly $\alpha$  nebulae attributed to gravitational cooling are usually extremely broad ( $FWHM \sim 1000 \text{ km s}^{-1}$ ), which differentiates them from LyC-leaking candidates, as well as images, with extended Ly $\alpha$  emission over several tens of kpc. Faucher-Giguère et al. (2010) computed the Ly $\alpha$  spectra of cold streams, which they find double-peaked, almost symmetrical (note that the IGM was not included in these calculations), and broad.

### 3. Comparison with other leaking indicators

To compare our theoretical prediction with observations, we now examine low-redshift objects from the literature for which direct Lyman continuum escape has been detected or which are considered candidates for LyC leakage on the basis of indirect indicators. Because possibilities for directly probing the ionising continuum in nearby galaxies have been limited to the archival FUSE data, indirect methods have been used frequently. These mainly include the measurement of saturation in the UV absorption lines of metals in their low-ionisation states, which form in the H $\text{I}$  regions. Residual flux in the lines indicates low optical depth or incomplete covering of the UV-light source (e.g. Heckman et al. 2001; Jones et al. 2013). Independently, the  $[\text{O III}]\lambda\lambda 4959, 5007/[\text{O II}]\lambda\lambda 3726, 3729$  line ratio has been proposed as a LyC optical-depth indicator (Jaskot & Oey 2013; Nakajima & Ouchi 2014). In density-bounded H $\text{II}$  regions, the

$[\text{O III}]$  excitation zones are expected to be largely unaffected, whereas the outer  $[\text{O II}]$  zones will be truncated, resulting in high  $[\text{O III}]/[\text{O II}]$  ratios (Kewley et al. 2013).

Our sample was selected from Bergvall et al. (2006); Heckman et al. (2011); Leitert et al. (2013). To this, we added Tol 1214–277 and GP1219+15, which show a Ly $\alpha$  profile that is highly suggestive of Lyman-continuum leakage according to our predictions in Sects. 2.3 and 2.2. The low-redshift data are convenient for this study because of the availability of high-resolution Ly $\alpha$  spectra and the rich ancillary data. Ly $\alpha$  spectral properties of the sample are summarised in Table 1, together with the other criteria used for identification of possible LyC leakage. Column 2 indicates  $f_{\text{esc}}^{\text{LyC}}$  measured by direct Lyman-continuum-emission detection; Col. 3 gives  $f_{\text{esc}}^{\text{LyC}}$  deduced from the UV covering fraction estimated from the LIS absorption lines; Col. 4 lists the observed  $[\text{O III}]\lambda 5007/[\text{O II}]\lambda\lambda 3726, 3729$  ratio, Col. 5 gives Ly $\alpha$  peak offset, and Col. 6 shows the peak separation for double-peaked profiles.

#### 3.1. Redshift and Ly $\alpha$ peak measurements

We present the UV Ly $\alpha$  line profiles of 11 objects in Figs. 6, 7, and 8 (Table 1 contains 12 entries, but the spectrum of Tol 1247–232 will be part of a detailed study of Puschnig et al. in prep). The data were mostly observed with HST/COS, one object was observed with HST/GHRs (Tol1214–277), and they were retrieved from the MAST multi-mission catalogue. We box-car smoothed the archival data to the nominal resolution of each of the spectrographs (COS  $R = 20\,000$  for a point source, GHRs  $R = 2000$ ). However, our sources are not point-like, and we estimate the real spectral resolution of COS Ly $\alpha$  to be  $\sim 100 \text{ km s}^{-1}$ , or  $R \sim 3000$  (Orlitova et al. in prep). We measured the main red Ly $\alpha$  peak offset ( $v_{\text{peak}}$ ) from the systemic velocity (Col. 5 of Tab. 1) and the separation  $S_{\text{peak}}$  of the main red and blue Ly $\alpha$  peaks of the double-peaked profiles (Col. 6 of Table 1). The main peak was defined as the flux maximum in each case (with no fitting performed). We comment on the cases where other significant peaks are present, especially if they are located closer to the systemic redshift, in the description of individual objects. Accurate systemic redshifts are necessary to reliably determine  $v_{\text{peak}}$ . We assume that the intrinsic Ly $\alpha$  is formed in the same H $\text{II}$  regions and by the same mechanisms as H $\alpha$  and other Balmer lines, and therefore redshifts derived from the optical emission lines are relevant. Where available, we applied SDSS emission-line redshifts. For objects outside the SDSS database (Haro 11, Tol 1214–277 and Tol 1247–232), we adopted emission-line redshifts with the smallest error bars available through the NED database (see references in Table 1 and Fig. 6). The uncertainties in the measured peak positions are mainly due to the redshift errors, the noise, and the peak irregular shapes. We checked that errors in wavelength calibration contribute less than  $10 \text{ km s}^{-1}$ .

#### 3.2. Haro 11 and Tol 1247–232

Haro 11 is a known LyC leaker with  $f_{\text{esc}}(\text{LyC}) \sim 3\%$  measured in the FUSE spectra (Bergvall et al. 2006; Leitert et al. 2013). It is a blue compact galaxy, and its optical, UV, and Ly $\alpha$  morphologies were studied with HST in Kunth et al. (2003); Hayes et al. (2007), and Östlin et al. (2009). Knot C was found to have  $\text{Ly}\alpha/\text{H}\alpha \sim 10$ , indicating a direct Ly $\alpha$  escape from this region through holes or an optically thin medium. The galaxy is composed of three major condensations (knots). Cold gas observa-



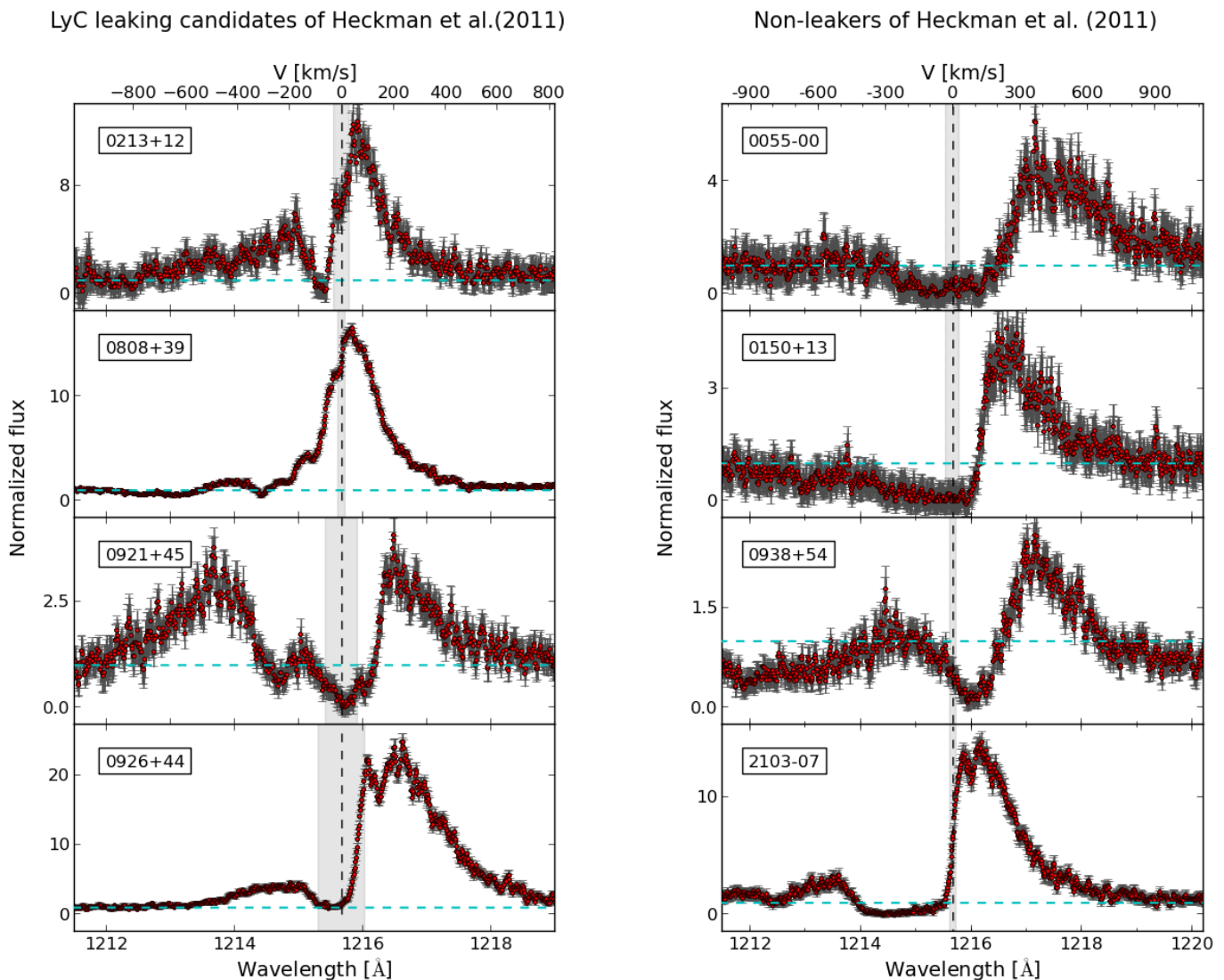


**Fig. 7.** Ly $\alpha$  profiles of LyC leaking (left) vs non-leaking candidates (right) from the sample of Heckman et al. (2011). The data have been smoothed to the nominal COS resolution (i.e.  $R = 20\,000$  for a point source). The systemic redshifts and their errors (grey shaded area in each plot) were derived from SDSS emission lines. The blue horizontal line denotes the continuum level. The signal-to-noise differences across the sample reflect both the redshifts and the intrinsic properties of the galaxies as Ly $\alpha$  sources.

tions through the Na I D line by Sandberg et al. (2013) suggest that the ISM is clumpy. The Ly $\alpha$  profile of knot C has recently been acquired with HST/COS (GO 13017, PI: T.Heckman, top panel of Fig. 6). It presents a standard asymmetric, redshifted line with  $v_{\text{peak}} = 115 \pm 50 \text{ km s}^{-1}$ . It is therefore just compatible with our prediction of LyC escape from a uniform medium of low column density, which is indicated by  $v_{\text{exp}} \lesssim 150 \text{ km s}^{-1}$ . Its  $[\text{O III}]/[\text{O II}] \sim 1.4$  (Guseva et al. 2012) ratio is moderate, as is its LyC escape fraction  $f_{\text{esc}}^{\text{LyC}} = 0.032$  derived from direct LyC measurement, and  $f_{\text{esc}}^{\text{LyC}} = 0.024$  derived from the LIS absorption lines (Leitet et al. 2013).

Tol 1247–232, the second-best candidate for LyC leakage, with a direct detection of non-zero Lyman continuum with FUSE (Leitet et al. 2013), has recently been observed with HST/COS (GO 13027, PI: G.Östlin, Puschign et al. in prep). The Ly $\alpha$  profile is similar to that of Haro 11, but broader, and peaks around  $v_{\text{peak}} = 150 \pm 70 \text{ km s}^{-1}$ , (marginally) compatible with  $v_{\text{peak}} \leq 150 \text{ km s}^{-1}$ . Its  $[\text{O III}]/[\text{O II}] \sim 3.4$  is the third-highest value

of our sample. The covering fraction of its LIS absorption lines remains to be determined from the new COS observations.

### 3.3. Tol 1214–277

Tol 1214–277 is a low-metallicity, compact blue dwarf galaxy (Thuan & Izotov 1997). It was unfortunately not observed with FUSE. However, its Ly $\alpha$  emission profile, observed with HST/GHRS (bottom panel of Fig. 6, see also Thuan & Izotov 1997; Mas-Hesse et al. 2003), peaks at the systemic velocity, it is thus a nice example of  $v_{\text{peak}} \sim 0$ . The Ly $\alpha$  profile seems to be composed of three sub-peaks, similar to the spectrum emerging from a static medium with a covering fraction  $\text{CF} = 0.90$  presented in the left panel of Fig. 4 (see also the triple-peaked profiles predicted by Behrens et al. 2014). A spectrum with higher resolution would be needed for a better understanding of the profile. However, the important feature is the profile centred on the systemic redshift, which cannot be reproduced by any model out

**Table 1.** Compilation of several indicators for LyC leakage from the low-redshift sample of candidate and confirmed LyC leakers<sup>(1)</sup>.

object ID*	$f_{\text{esc}}^{\text{LyC}}$ from direct LyC detection <sup>a</sup>	$f_{\text{esc}}^{\text{LyC}}$ from UV covering fraction <sup>b</sup>	[O III]/[O II] <sup>c</sup>	$v_{\text{peak}}(\text{Ly}\alpha)$ [km s <sup>-1</sup> ] <sup>d</sup>	Ly $\alpha$ peak separation [km s <sup>-1</sup> ]
Tol 1247–232	0.024	–	$3.4 \pm 0.6$	$130 \pm 70$	$500 \pm 30$
Haro 11	0.032	0.024 <sup>a</sup>	$1.5 \pm 0.2$	$110 \pm 60$	–
Tol 1214–277	> 0 suspected <sup>e</sup>	> 0 suspected <sup>f</sup>	$15 \pm 3$	$60 \pm 60$	$650 \pm 50$
GP 1219+15	> 0 suspected <sup>e</sup>	–	$10.2 \pm 0.3$	$170 \pm 20$	$270 \pm 20$
0213+12	–	0.05	$0.8 \pm 0.4$	$70 \pm 30$	$230 \pm 10$
0808+39	–	0.12	$0.60 \pm 0.08$	$30 \pm 20$	$450 \pm 30$
0921+45	–	0.04	$0.28 \pm 0.03$	$240 \pm 60$	$690 \pm 10$
0926+44	–	0.40	$3.2 \pm 0.1$	$280 \pm 90$	$450 \pm 50$
0055–00	–	< 0.01	$1.52 \pm 0.03$	$370 \pm 30$	$900 \pm 50$
0150+13	–	< 0.01	$0.79 \pm 0.02$	$260 \pm 50$	–
0938+54	–	< 0.05	$1.97 \pm 0.04$	$350 \pm 30$	$550 \pm 100$
2103–07	–	< 0.01	$0.52 \pm 0.03$	$130 \pm 20$	$700 \pm 50$

<sup>(1)</sup> from Bergvall et al. (2006); Heckman et al. (2011); Leitert et al. (2013) plus Tol 1214–277 (Thuan & Izotov 1997; Mas-Hesse et al. 2003), and GP1291+15 (Cardamone et al. 2009), for which medium-resolution Ly $\alpha$  spectra are available. Below the horizontal line we also list four non-leakers from the sample of Heckman et al. (2011) for comparison. <sup>(\*)</sup> Official catalogue names: Tol 1247–232, Haro 11, Tol 1214–277, SDSSJ121903.98+152608.5, SDSSJ021348.53+125951.4, SDSSJ080844.26+394852.3, SDSSJ092159.39+450912.3, SDSSJ092600.40+442736.1, SDSSJ005527.46–002148.7, SDSSJ015028.40+130858.3, SDSSJ093813.49+542825.0, SDSSJ210358.74–072802.4 <sup>(a)</sup> From Leitert et al. (2013). <sup>(b)</sup> Taken from Heckman et al. (2011) if not indicated otherwise. <sup>(c)</sup> [O III] $\lambda$ 5007/[O II] $\lambda$ 3726, 3729 derived from SDSS data for Heckman et al. (2011) sample and for the green peas; from Terlevich et al. (1991) for Tol 1214–277 and Tol 1247–232; and from Guseva et al. (2012) for Haro 11. <sup>(d)</sup> Measured main Ly $\alpha$  peak offset. Systemic emission-line redshifts adopted from the SDSS for the sample of Heckman et al. (2011) and for the green peas; from the 6dF survey of Haro 11; from Pustilnik & Martin (2007) for Tol 1214–277; from the H $\alpha$  line (E. Freeland, private communication) for Tol1247-232. <sup>(e)</sup> Based on Ly $\alpha$  in this study; cf. also Mas-Hesse et al. (2003). <sup>(f)</sup> Thuan & Izotov (1997)

of our grid of > 6000 radiation transfer models for homogeneous shells (Schaerer et al. 2011). We can reproduce the external peaks alone with a static homogeneous model. The central peak can either result from a high-velocity component or from clumpy (riddled) medium with incomplete covering, which allows for LyC leakage (as in Fig. 4).

The C II  $\lambda$ 1335 absorption line shows two velocity components, one centred on the systemic velocity, the other blueshifted by 950 km s<sup>-1</sup>. The rapid motions can contribute to the Ly $\alpha$  escape at systemic velocity. However, both C II components are unsaturated, which may indicate a non-uniform coverage of neutral gas along the line of sight, which would favour our scenario of LyC escape through holes. The same qualitative conclusion was reached by Thuan & Izotov (1997).

An alternative interpretation was provided by Mas-Hesse et al. (2003). They suggested that the central component corresponds to direct Ly $\alpha$  emission from an ionised cavity, while the two additional emission peaks originate from ionisation fronts trapped within the expanding shell (both approaching and receding). In this case, the outflow velocity is predicted to be traced by the lateral peaks at  $v_{\text{exp}} \approx 300$  km s<sup>-1</sup>.

The observed ratio of [O III]/[O II]  $\sim 15$  of Tol 1214–277 is very high, suggesting high ionisation (and/or low metallicity) of the H II region (Kewley & Dopita 2002; Kewley et al. 2013; Jaskot & Oey 2013; Nakajima & Ouchi 2014).

### 3.4. Lyman-break analogues

Heckman et al. (2011) have identified three LyC-leaking candidates among their eight Lyman-break analogues (LBAs) that were observed with HST/COS. They defined the LyC-leaking candidates as those that show incomplete covering of the far-UV source by neutral gas clouds (derived from the UV LIS absorp-

tion lines), and whose UV morphology is dominated by a central compact source. They did not consider 0926+44 a leaking candidate although it has the lowest UV-covering fraction of the entire sample as a result of the absence of the dominant central core. We here consider this fourth object together with the other three leaking candidates and show their Ly $\alpha$  profiles in the left panel of Fig. 7. The remaining four non-leaking galaxies from their sample are shown in the right panel of Fig. 7.

We find that all of the objects identified as potential leakers have unusual rather complicated Ly $\alpha$  spectra with bumps and substructures in the main peaks that are impossible to model completely with radiative transfer models in homogeneous expanding shells. In contrast, the non-leaking objects have classical P Cygni-type Ly $\alpha$  profiles. Two leaking candidates (0213+12 and 0808+39) have a very low  $v_{\text{peak}}$  ( $\sim 70$  km s<sup>-1</sup> and  $\sim 30$  km s<sup>-1</sup>, respectively, see Table 1) and in addition show a subpeak at the systemic redshift, which may indicate Ly $\alpha$  transfer through a riddled ISM. The subpeak in 0213+12 is weak, but the main double-peak structure is narrow and the object could also be classified as a LyC-leaking candidate with a low column density. The Ly $\alpha$  profile of 0926+44 has a maximum at  $280 \pm 90$  km s<sup>-1</sup> and a blue peak separated by  $\sim 450$  km s<sup>-1</sup>, which excludes LyC leakage. However, a strong subpeak is present at  $100 \pm 90$  km s<sup>-1</sup>, which fits our LyC leaking criteria. The Ly $\alpha$  spectrum thus seems to be composed of two components that can either be due to complex morphology and kinematics of the galaxy (Basu-Zych et al. 2009; Gonçalves et al. 2010) or to high-velocity outflows (Heckman et al. 2011) and is not straightforward to interpret.

Three of the four leaking candidates reported by Heckman emit significant flux bluewards of the systemic redshift, as pointed out by Heckman et al. (2011), but the separation between the peaks is too high to fit our predictions of leakage

through the optically thin scenario, except for 0213+12. The object 0921+45 of the leaking candidates listed by Heckman et al. does not meet our criteria for LyC leakage because of its large Ly $\alpha$  absorption trough around the systemic redshift, indicating large amounts of neutral gas and dust. It has recently been observed in the LyC continuum, and its absolute escape fraction is indeed low ( $\sim 1\%$ ), although the relative escape is higher ( $\sim 21\%$  Borthakur et al. 2014). Of the non-leakers, three out of four have  $v_{\text{peak}} \gg 150 \text{ km s}^{-1}$  and no Ly $\alpha$  escape bluewards of the systemic redshift. Indeed, these objects present a broad absorption bluewards of the systemic redshift. As an exception among the non-leakers of Heckman, 2103–07 has  $v_{\text{peak}} \leq 150 \text{ km s}^{-1}$  and its Ly $\alpha$  red peak has a substructure that could also be interpreted as a subpeak at  $v \sim 50 \text{ km s}^{-1}$ . However, the LIS absorption lines are saturated and indicate no LyC escape. In addition, its large Ly $\alpha$  absorption trough suggests a large amount of dust. The low  $v_{\text{peak}}$  does not contradict our LyC prediction criteria because low  $v_{\text{peak}}$  values can also appear in high column density objects (see Fig. 2), and the  $v_{\text{peak}}$  alone is not sufficient to predict the LyC leaking.

The [O III]/[O II] ratios are all below  $\sim 3$  for both leakers and non-leakers, and the mean [O III]/[O II] values are almost identical ( $\langle [\text{O III}]/[\text{O II}] \rangle = 1.22$  for leakers and 1.20 for non-leakers). None of the objects in the sample of Heckman have the extreme [O III]/[O II] ratios reported in Jaskot & Oey (2013) to potentially trace density bounded H II regions.

### 3.5. Other leaking candidates in the literature

Among the LyC-leaking candidates presented in Leitert et al. (2013), ESO 338–IG04 and SBS 0335–052 are the two with the strongest continuum escape fractions derived from the UV LIS lines. They were both observed with FUSE. Unfortunately, they are so close in redshift that it is impossible to constrain the LyC escape from these observations. Their [O III]/[O II] ratios are  $\sim 4$  and  $\sim 12$ , respectively (Guseva et al. 2012; Izotov et al. 2009). However, SBS 0335–052 is a Ly $\alpha$  absorber (Thuan & Izotov 1997), and therefore our Ly $\alpha$  emission profile diagnostics are not applicable. It is the second-most metal-poor blue compact dwarf known to date, and therefore its [O III]/[O II] ratio probably results from the extremely low metallicity (see e.g. Kewley et al. 2013, for a discussion of this effect). It is embedded in an enormous H I cloud, and thus we believe that SBS 0335–052 is not a good leaking candidate.

For ESO 338–IG04, we have a UV slit spectrum observed with HST/STIS, but unfortunately in the low-resolution mode ( $R = 1000$ ). The analysis of spectra from the emission knots (Hayes et al. 2005) shows great spatial variability, ranging from absorption to emission. The Ly $\alpha$  spectrum that emerges from knot D shows  $v_{\text{peak}} \sim 0$  and therefore seems compatible with LyC leakage according to our Ly $\alpha$  diagnostics presented in this study. However, a high-resolution spectrum is necessary for a confirmation.

Recently, UV spectra of green peas (Cardamone et al. 2009) acquired with HST/COS have become available through the MAST archive (GO 12928, PI: A.Henry, GO 13293, PI: A.Jaskot, Jaskot & Oey 2014). We have analysed several of their Ly $\alpha$  profiles and are working on modelling them with the radiation transfer code McLya (Orlitová et al. in prep). We find that the object with the highest [O III]/[O II] ratio ( $\sim 10$ ), GP 1219+1526, has a narrow double-peak Ly $\alpha$  profile ( $S_{\text{peak}} \sim 270 < 300 \text{ km s}^{-1}$ ,  $v_{\text{peak}} \sim 170 \pm 20 \text{ km s}^{-1}$ , see Fig. 8), indicating probable LyC leaking from this object.

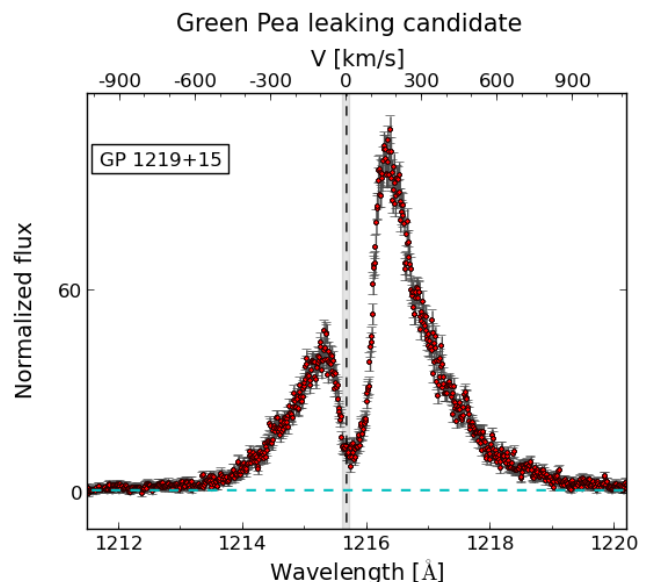


**Fig. 8.** Green pea 1219+15 is a good candidate for LyC leaking according to our Ly $\alpha$  diagnostics because the double peaks are separated by  $\sim 270 < 300 \text{ km s}^{-1}$ .

A unique test of our LyC-Ly $\alpha$  connection is possible thanks to the active galactic nuclei (AGN), where strong flux of ionising continuum is known to escape from type 1 sources, while it is missing in type 2 AGN. We therefore expect a difference between Ly $\alpha$  spectra in the two types. And indeed, in agreement with our predictions, Ly $\alpha$  spectra of Seyfert 1 galaxies and type 1 quasars in low and high redshift show strong Ly $\alpha$  emission lines at systemic velocity (Gregory et al. 1982; Rudy et al. 1988; Crenshaw et al. 1999; Kraemer et al. 2001; Shull et al. 2012; Herenz et al. 2015). We examined the spectra directly in the MAST archive, where possible. These sources include types 1–1.8, which means that they have a partially obscured AGN, in line with our models. NGC 4303, the only true type 2 Seyfert galaxy for which we have found a Ly $\alpha$  spectrum, has a P Cygni profile with a redshifted peak (Colina et al. 2002).

## 4. Discussion

In the data available with low redshift, we have seen that it is rare to find spectra with the Ly $\alpha$  peak centred on systemic redshift, suggesting a clumpy ISM. Instead, our criteria related to the low column density neutral ISM were used more frequently. We found that the two objects with directly detected LyC, that is, Haro 11 and Tol 1247–232 (Leitert et al. 2013), indeed have Ly $\alpha$  spectra characterised by  $v_{\text{peak}} < 150 \text{ km s}^{-1}$ , as predicted by our models. Therefore, the Ly $\alpha$  spectral diagnostics do not contradict the LyC measurements.

Among the candidates identified by weak LIS absorption lines, we found Ly $\alpha$  spectra with interesting features, and at least some of them would be classified as LyC-leakage candidates according to our criteria (Tol 1214–277, LBA 0213+12, LBA 0808+39, GP 1219+15). Consistently, the objects where LyC leakage was excluded by the LIS absorption lines method show Ly $\alpha$  spectra that clearly result from high column densities of neutral gas and/or dust. The cases in which weak LIS absorption lines were detected, but where at the same time our criteria exclude LyC leakage, have unusual Ly $\alpha$  spectra (LBA 0921+45, LBA 0926+44), and seem to have complex galaxy morphologies (Gonçalves et al. 2010) and would need a more detailed study.

Therefore, based on the available data sample, we are confident that our theoretical prediction of Ly $\alpha$  features indicating LyC leakage is a viable approach for identifying leaking candidates at both low and high redshift.

We have also described possible limitations of our method: 1) relatively high spectral resolution ( $R > 4000$ ) is required for a clear interpretation of the spectral profile; 2) redshift precision is crucial for correctly determining the Ly $\alpha$  peak offset; 3) one of our criteria relies on double-peaked Ly $\alpha$  profiles, which are rare; 4) our method only indicates leaking candidates and cannot alone prove the LyC leakage. Detailed modelling of the individual Ly $\alpha$  spectra will help to distinguish between the cases of Ly $\alpha$  peaks close to the systemic redshift that are due to the ISM that is optically thin for LyC and those that are only transparent to Ly $\alpha$  as a result of fast outflows or other conditions. However, the ultimate confirmation of LyC leakage for every selected candidate must come from the direct LyC detection. We have shown that our Ly $\alpha$  spectral criteria can reliably identify non-leakers in which LyC leakage is excluded.

Erb et al. (2010, 2014); Heckman et al. (2011) concluded based on observational results that Ly $\alpha$  flux bluewards of the systemic redshift is related to the LyC leakage. This is similar to our criteria in the case where the neutral ISM is clumpy and the observed Ly $\alpha$  profile is centred on the systemic redshift. However, the blue-flux objects also contain those that have double peaks arising from a static ISM. Our method provides a theoretical background to these observational findings and sets clear criteria for LyC signatures in the Ly $\alpha$  profiles.

A comparison with [O III]/[O II] is less straightforward. Galaxies with [O III]/[O II]  $< \sim 4$  are characterised by a wide spread in  $v_{\text{peak}}$  and  $S_{\text{peak}}$ , whereas only a few objects have larger [O III]/[O II]. The wide spread is consistent with results reported by Nakajima & Ouchi (2014), who showed that [O III]/[O II] as a LyC diagnostics is strongly affected by the degeneracy between metallicity and ionisation parameter. Large statistical galaxy samples are needed to test the correlation between [O III]/[O II] and the Ly $\alpha$  profile parameters. See also Stasinska et al. (2015).

Obviously, larger galaxy samples with both high-resolution Ly $\alpha$  spectra and measured  $f_{\text{esc}}(\text{LyC})$  are needed to derive statistically robust conclusions. However, we believe that our theoretical predictions of Sect. 2 (i.e., low  $v_{\text{peak}}$  and  $S_{\text{peak}}$ , or Ly $\alpha$  peak at systemic redshift for LyC leaking candidates) have been shown to be useful based on the presented HST archive sample. Several HST/COS programs that investigate the Lyman-alpha spectra and LyC escape fraction from local galaxies are ongoing. By the end of 2015, the number of HST/COS Ly $\alpha$  spectra available will be  $> 100$ , which will provide an important sample size, and hopefully, new insights into the LyC-leakage problem will be gained.

## 5. Conclusions

We have carried out Ly $\alpha$  radiation transfer simulations in two idealised configurations of LyC-leaking star-forming galaxies:

1. Homogeneous spherically expanding ISM shells with a central Ly $\alpha$  source, but with extremely low column densities ( $N_{\text{HI}} \leq 10^{18} \text{ cm}^{-2}$ ),
2. clumpy spherical shells with a non-unity covering fraction, called riddled ionisation-bounded H II regions.

In both cases, we find that the emerging Ly $\alpha$  spectrum has remarkable features that may be possible to identify in observed Ly $\alpha$  spectra, assuming that the Ly $\alpha$  spectrum from a galaxy

may be dominated by the Ly $\alpha$  component emerging from LyC-leaking star clusters. According to the first scenario, the Ly $\alpha$  spectrum will have a classical asymmetric redshifted profile, but with a small shift ( $v_{\text{peak}} \leq 150 \text{ km s}^{-1}$ ). According to the second scenario, the main feature is a peak at the systemic redshift of the star cluster, with, as a consequence, a non-zero flux bluewards of the Ly $\alpha$  line centre. These two signatures may be used to distinguish or select leaking candidates at all redshifts for objects with high spectral resolution and well-determined systemic redshift.

We have examined how these diagnostics compare with observed Ly $\alpha$  spectra from the local Universe where either the LyC escape fraction has been directly measured (Bergvall et al. 2006; Leitet et al. 2013) or has been derived from LIS absorption lines studies (Heckman et al. 2011). We also tested our predictions against a sample of non-leaking galaxies of the same team. Although the number of objects is very small to derive statistically robust conclusions, the expected trends seem to be at work ( $v_{\text{peak}}$  and  $S_{\text{peak}}$  smaller for leakers than non-leakers).

We proposed two additional galaxies as good candidates for LyC leaking: GP 1219+1526, based on the small separation of the peaks in its Ly $\alpha$  profile, and a high [O III]/[O II] ratio, could be leaking according to our first scenario of a density-bounded region; Tol 1214–277, described in Thuan & Izotov (1997), based on its very peculiar Ly $\alpha$  spectral shape (symmetrical triple peak with the main peak at  $v_{\text{peak}} = 0$ ), and indications of non-total coverage of LIS absorption lines, could be leaking from a riddled ISM.

There are well-known objects in the local Universe from which a strong LyC flux is detected, belonging to the family of AGNs. As another validation of our diagnostics, we verified in the literature that Ly $\alpha$  spectra from these known LyC leakers are in emission, and peak at the line centre.

Our predictions need to be tested on larger samples with well-determined systemic redshifts and high spectral resolution Ly $\alpha$  profiles. But apparently a small shift of the maximum of the Ly $\alpha$  profile with respect to the systemic redshift ( $v_{\text{peak}} \leq 150 \text{ km s}^{-1}$ ) may be a good proxy for a non-zero escape fraction of ionising radiation from galaxies.

*Acknowledgements.* We thank Florent Duval for sharing radiation transfer and clumpy geometry models from Duval et al. (2014). We are grateful to the anonymous referee and to Miguel Mas Hesse for their thoughtful comments that helped us improve the paper. A.V. is supported by a Fellowship "Boursière d'Excellence" of Geneva University. I.O. acknowledges the support from the Sciex fellowship of the Rectors' Conference of Swiss Universities, and the grant 14-20666P of Czech Science Foundation, together with the long-term institutional grant RVO:67985815. M.H. acknowledges the support of the Swedish Research Council, Vetenskapsrådet, and the Swedish National Space Board (SNSB). This work used NASA/ESA HST archival data from programmes GO 6678, GO 9036, GO 11727, GO 12928, GO 13017, and GO 13027. All of the data presented in this paper were obtained from Mikulski Archive for Space Telescopes (MAST). STScI is operated by the Association of Universities for Research in Astronomy, Inc., under NASA contract NAS5-26555. Support for MAST for non-HST data is provided by the NASA Office of Space Science via grant NNX13AC07G and by other grants and contracts. We made use of the SAO/NASA Astrophysics Data System (ADS), the NASA/IPAC Extragalactic Database (NED), and the Image Reduction and Analysis Facility (IRAF), distributed by the National Optical Astronomy Observatories.

## References

- Alavi, A., Siana, B., Richard, J., et al. 2014, ApJ, 780, 143  
 Basu-Zych, A. R., Gonçalves, T. S., Overzier, R., et al. 2009, ApJ, 699, L118  
 Behrens, C., Dijkstra, M., & Niemeyer, J. C. 2014, A&A, 563, A77  
 Bergvall, N., Zackrisson, E., Andersson, B.-G., et al. 2006, A&A, 448, 513  
 Bielby, R. M., Shanks, T., Weilbacher, P. M., et al. 2011, MNRAS, 414, 2  
 Borthakur, S., Heckman, T. M., Leitherer, C., & Overzier, R. A. 2014, Science, 346, 216

- Bradshaw, E. J., Almaini, O., Hartley, W. G., et al. 2013, *MNRAS*, 433, 194
- Calzetti, D., Armus, L., Bohlin, R. C., et al. 2000, *ApJ*, 533, 682
- Cantalupo, S., Lilly, S. J., & Haehnelt, M. G. 2012, *MNRAS*, 425, 1992
- Cantalupo, S., Porciani, C., Lilly, S. J., & Miniati, F. 2005, *ApJ*, 628, 61
- Cardamone, C., Schawinski, K., Sarzi, M., et al. 2009, *MNRAS*, 399, 1191
- Chonis, T. S., Blanc, G. A., Hill, G. J., et al. 2013, *ApJ*, 775, 99
- Christensen, L., Laursen, P., Richard, J., et al. 2012a, *MNRAS*, 427, 1973
- Christensen, L., Richard, J., Hjorth, J., et al. 2012b, *MNRAS*, 427, 1953
- Colina, L., Gonzalez Delgado, R., Mas-Hesse, J. M., & Leitherer, C. 2002, *ApJ*, 579, 545
- Cooke, J., Ryan-Weber, E. V., Garel, T., & Díaz, C. G. 2014, *MNRAS*, 441, 837
- Cowie, L. L., Barger, A. J., & Trouille, L. 2009, *ApJ*, 692, 1476
- Crenshaw, D. M., Kraemer, S. B., Boggess, A., et al. 1999, *ApJ*, 516, 750
- Deharveng, J.-M., Buat, V., Le Brun, V., et al. 2001, *A&A*, 375, 805
- Dessauges-Zavadsky, M., D'Odorico, S., Schaerer, D., et al. 2010, *A&A*, 510, A26+
- Dijkstra, M., Haiman, Z., & Spaans, M. 2006, *ApJ*, 649, 14
- Dijkstra, M. & Kramer, R. 2012, *MNRAS*, 424, 1672
- Dijkstra, M., Wyithe, S., Haiman, Z., Mesinger, A., & Pentericci, L. 2014, *MNRAS*, 440, 3309
- Dressler, A., Henry, A., Martin, C. L., et al. 2014, *ArXiv e-prints*
- Dressler, A., Martin, C. L., Henry, A., Sawicki, M., & McCarthy, P. 2011, *ApJ*, 740, 71
- Duval, F., Schaerer, D., Östlin, G., & Laursen, P. 2014, *A&A*, 562, A52
- Ellis, R. S., McLure, R. J., Dunlop, J. S., et al. 2013, *ApJ*, 763, L7
- Erb, D. K., Pettini, M., Shapley, A. E., et al. 2010, *ApJ*, 719, 1168
- Erb, D. K., Steidel, C. C., Trainor, R. F., et al. 2014, *ApJ*, 795, 33
- Faucher-Giguère, C.-A., Kereš, D., Dijkstra, M., Hernquist, L., & Zaldarriaga, M. 2010, *ApJ*, 725, 633
- Ferrara, A. & Loeb, A. 2013, *MNRAS*, 431, 2826
- Fontanot, F., Cristiani, S., & Vanzella, E. 2012, *MNRAS*, 425, 1413
- Gawiser, E., van Dokkum, P. G., Gronwall, C., et al. 2006, *ApJ*, 642, L13
- Gonçalves, T. S., Basu-Zych, A., Overzier, R., et al. 2010, *ApJ*, 724, 1373
- Gregory, S., Ptak, R., & Stoner, R. 1982, *ApJ*, 261, 30
- Grimes, J. P., Heckman, T., Aloisi, A., et al. 2009, *ApJS*, 181, 272
- Gronke, M. & Dijkstra, M. 2014, *MNRAS*, 444, 1095
- Guaita, L., Acquaviva, V., Padilla, N., et al. 2011, *ApJ*, 733, 114
- Guaita, L., Gawiser, E., Padilla, N., et al. 2010, *ApJ*, 714, 255
- Guseva, N. G., Izotov, Y. I., Fricke, K. J., & Henkel, C. 2012, *A&A*, 541, A115
- Hayes, M., Östlin, G., Atek, H., et al. 2007, *MNRAS*, 382, 1465
- Hayes, M., Östlin, G., Mas-Hesse, J. M., et al. 2005, *A&A*, 438, 71
- Hayes, M., Scarlata, C., & Siana, B. 2011, *Nature*, 476, 304
- Heckman, T. M., Borthakur, S., Overzier, R., et al. 2011, *ApJ*, 730, 5
- Heckman, T. M., Sembach, K. R., Meurer, G. R., et al. 2001, *ApJ*, 558, 56
- Herenz, E. C., Wisotzki, L., Roth, M., & Anders, F. 2015, *ArXiv e-prints*
- Hu, E. M., Cowie, L. L., Barger, A. J., et al. 2010, *ApJ*, 725, 394
- Iwata, I., Inoue, A. K., Matsuda, Y., et al. 2009, *ApJ*, 692, 1287
- Izotov, Y. I., Guseva, N. G., Fricke, K. J., & Papaderos, P. 2009, *A&A*, 503, 61
- Izotov, Y. I., Guseva, N. G., & Thuan, T. X. 2011, *ApJ*, 728, 161
- Jaskot, A. E. & Oey, M. S. 2013, *ApJ*, 766, 91
- Jaskot, A. E. & Oey, M. S. 2014, *ApJ*, 791, L19
- Jiang, L., Egami, E., Fan, X., et al. 2013a, *ApJ*, 773, 153
- Jiang, L., Egami, E., Mechtley, M., et al. 2013b, *ApJ*, 772, 99
- Jones, T. A., Ellis, R. S., Schenker, M. A., & Stark, D. P. 2013, *ApJ*, 779, 52
- Karman, W., Caputi, K. I., Trager, S. C., Almaini, O., & Cirasuolo, M. 2014, *A&A*, 565, A5
- Kewley, L. J. & Dopita, M. A. 2002, *ApJS*, 142, 35
- Kewley, L. J., Dopita, M. A., Leitherer, C., et al. 2013, *ApJ*, 774, 100
- Kollmeier, J. A., Zheng, Z., Davé, R., et al. 2010, *ApJ*, 708, 1048
- Kraemer, S. B., Crenshaw, D. M., & Gabel, J. R. 2001, *ApJ*, 557, 30
- Kulas, K. R., Shapley, A. E., Kollmeier, J. A., et al. 2012, *ApJ*, 745, 33
- Kunth, D., Leitherer, C., Mas-Hesse, J. M., Östlin, G., & Petrosian, A. 2003, *ApJ*, 597, 263
- Laursen, P., Duval, F., & Östlin, G. 2013, *ApJ*, 766, 124
- Laursen, P., Sommer-Larsen, J., & Razoumov, A. O. 2011, *ApJ*, 728, 52
- Lee, J. C., Gil de Paz, A., Tremonti, C., et al. 2009, *ApJ*, 706, 599
- Leitet, E., Bergvall, N., Hayes, M., Linné, S., & Zackrisson, E. 2013, *A&A*, 553, A106
- Leitet, E., Bergvall, N., Piskunov, N., & Andersson, B.-G. 2011, *A&A*, 532, A107
- Leitherer, C., Ferguson, H. C., Heckman, T. M., & Lowenthal, J. D. 1995, *ApJ*, 454, L19
- Lidman, C., Hayes, M., Jones, D. H., et al. 2012, *MNRAS*, 420, 1946
- Malkan, M., Webb, W., & Konopacky, Q. 2003, *ApJ*, 598, 878
- Mas-Hesse, J. M., Kunth, D., Tenorio-Tagle, G., et al. 2003, *ApJ*, 598, 858
- Mostardi, R. E., Shapley, A. E., Nestor, D. B., et al. 2013, *ApJ*, 779, 65
- Nakajima, K. & Ouchi, M. 2014, *MNRAS*, 442, 900
- Nestor, D. B., Shapley, A. E., Kornei, K. A., Steidel, C. C., & Siana, B. 2013, *ApJ*, 765, 47
- Nestor, D. B., Shapley, A. E., Steidel, C. C., & Siana, B. 2011, *ApJ*, 736, 18
- Neufeld, D. A. 1990, *ApJ*, 350, 216
- Neufeld, D. A. 1991, *ApJ*, 370, L85
- Noterdaeme, P., Laursen, P., Petitjean, P., et al. 2012, *A&A*, 540, A63
- Ono, Y., Ouchi, M., Mobasher, B., et al. 2012, *ApJ*, 744, 83
- Östlin, G., Hayes, M., Kunth, D., et al. 2009, *AJ*, 138, 923
- Ouchi, M., Hamana, T., Shimasaku, K., et al. 2005, *ApJ*, 635, L117
- Ouchi, M., Shimasaku, K., Akiyama, M., et al. 2008, *ApJS*, 176, 301
- Pellegrini, E. W., Oey, M. S., Winkler, P. F., et al. 2012, *ApJ*, 755, 40
- Pentericci, L., Fontana, A., Vanzella, E., et al. 2011, *ApJ*, 743, 132
- Pentericci, L., Grazian, A., Scarlata, C., et al. 2010, *A&A*, 514, A64
- Pustilnik, S. A. & Martin, J.-M. 2007, *A&A*, 464, 859
- Robertson, B. E., Furlanetto, S. R., Schneider, E., et al. 2013, *ApJ*, 768, 71
- Rudy, R. J., Cohen, R. D., & Ake, T. B. 1988, *ApJ*, 332, 172
- Sandberg, A., Östlin, G., Hayes, M., et al. 2013, *A&A*, 552, A95
- Schaerer, D., Hayes, M., Verhamme, A., & Teyssier, R. 2011, *A&A*, 531, A12
- Schenker, M. A., Ellis, R. S., Konidaris, N. P., & Stark, D. P. 2014, *ApJ*, 795, 20
- Schenker, M. A., Robertson, B. E., Ellis, R. S., et al. 2013, *ApJ*, 768, 196
- Seaton, M. J. 1979, *MNRAS*, 187, 73P
- Shapley, A. E., Steidel, C. C., Pettini, M., & Adelberger, K. L. 2003, *ApJ*, 588, 65
- Shapley, A. E., Steidel, C. C., Pettini, M., Adelberger, K. L., & Erb, D. K. 2006, *ApJ*, 651, 688
- Shull, J. M., Stevans, M., & Danforth, C. W. 2012, *ApJ*, 752, 162
- Siana, B., Teplitz, H. I., Colbert, J., et al. 2007, *ApJ*, 668, 62
- Siana, B., Teplitz, H. I., Ferguson, H. C., et al. 2010, *ApJ*, 723, 241
- Stark, D. P., Ellis, R. S., Chiu, K., Ouchi, M., & Bunker, A. 2010, *MNRAS*, 408, 1628
- Stasinska, G., Izotov, Y., Morisset, C., & Guseva, N. 2015, *ArXiv e-prints*
- Steidel, C. C., Pettini, M., & Adelberger, K. L. 2001, *ApJ*, 546, 665
- Strömgren, B. 1939, *ApJ*, 89, 526
- Tapken, C., Appenzeller, I., Noll, S., et al. 2007, *A&A*, 467, 63
- Terlevich, R., Melnick, J., Masegosa, J., Moles, M., & Copetti, M. V. F. 1991, *A&AS*, 91, 285
- Thuan, T. X. & Izotov, Y. I. 1997, *ApJ*, 489, 623
- Trainor, R. & Steidel, C. C. 2013, *ApJ*, 775, L3
- Vanzella, E., Grazian, A., Hayes, M., et al. 2010, *A&A*, 513, A20+
- Vanzella, E., Guo, Y., Giavalisco, M., et al. 2012, *ApJ*, 751, 70
- Verhamme, A., Schaerer, D., Atek, H., & Tapken, C. 2008, *A&A*, 491, 89
- Verhamme, A., Schaerer, D., & Maselli, A. 2006, *A&A*, 460, 397
- Wise, J. H. & Cen, R. 2009, *ApJ*, 693, 984
- Witt, A. N. & Gordon, K. D. 2000, *ApJ*, 528, 799
- Yajima, H., Choi, J.-H., & Nagamine, K. 2011, *MNRAS*, 412, 411
- Zackrisson, E., Inoue, A. K., & Jensen, H. 2013, *ApJ*, 777, 39
- Zheng, Z. & Miralda-Escudé, J. 2002, *ApJ*, 578, 33